ISSN: 0976-3031

Available Online at http://www.recentscientific.com

CODEN: IJRSFP (USA)

International Journal of Recent Scientific Research
Vol. 9, Issue, 8(A), pp. 28260-28269, August, 2018

International Journal of Recent Scientific Research

DOI: 10.24327/IJRSR

Research Article

USE OF KAOLINITE AS AN ADSORBENT: EQUILIBRIUM AND DYNAMICS OF ADSORPTION OF DIRECT RED 13 FROM AQUEOUS SOLUTION

Mohammed A. H. Dhaif Allah[1] and Akheel Ahmed Syed[2*]

[1]Department of Studies in Environmental Science, University of Mysore, Manasagangothri, Mysuru-570006, India
[2]Department of Studies in Chemistry, University of Mysore, Manasagangothri, Mysore - 570006, India

DOI: http://dx.doi.org/10.24327/ijrsr.2018.0908.2427

ARTICLE INFO

Article History:
Received 19th May, 2018
Received in revised form 5th June, 2018
Accepted 10th July, 2018
Published online 28th August, 2018

Key Words:

Adsorption isotherms, ANOVA, Direct Red 13, Fractional factorial experimental design, Kinetics, Kaolinite, Modeling

ABSTRACT

Adsorption efficiency of kaolinite to remove Direct Red 13, toxic andanionic bisazo dye, from aqueous solution has been attempted. The parameters tested and conditions optimized included initial concentration of DR13 (100 mg/L), agitation period (180 min), adsorbent dose (0.300 g/L), pH 7 as well as temperature (303K, 313K, 323K). Adsorption data were evaluated by using such isothermal models as Langmuir, Freundlich and Temkin. High correlation coefficient (R^2) was observed only with the Langmuir isotherm, and the monolayer adsorption capacity (*Qm*) observed was7.5 mg/g. Kinetic data has good agreement with pseudo-first order model. Fraction Factorial Experimental Design (FFED) and the analysis of variance (ANOVA) indicated maximum adsorption of 85 *mg/g* of the dye on the kaolinite. It was suggested that kaolinite can be used as low-cost adsorbent for DR13 removal from wastewater.

INTRODUCTION

Azo dyes are reactive dyes representing about 70% of all the dyes used in textile industries. Direct red 13 (DR13) is a benzidine-based anionic bisazo dye, which gets metabolized to benzidine, a known human carcinogen (Mall *et al*., 2005). Owing to structural stability of benzidine based azo dyes, DR13 which has structural similarity like Congo red, is likely to be highly resistant to microbial biodegradation.

The textile industry plays a major role in the economy. It is estimated that globally 280,000 tons of residual dyes are discharged as textile industrial effluent every year (Jin *et al*., 2007). This is because depending on the class of dye, the efficiency and efficacy of molecules attachment to the fabric vary from 98% for basic dyes to as low as 50% for reactive dyes, leading to severe wastage and hence contamination of surface and ground waters in the vicinity of dyeing industries (Neill *et al*., 1999). Industrial effluents containing synthetic dyes allegedly reduce light penetration in water bodies and affect the photosynthetic activity of aquatic flora, thereby severely affecting the food generation for aquatic organisms (Yao *et al*., 1999). Most of the dyes are toxic by themselves, but after being released into the aquatic environment, they may get converted into potentially carcinogenic amines and affect the ecosystem and human health.

By stringent government legislation textile industries are made to treat waste effluent to high standard. Removal of dyes from effluent is at present is achieved by physio-chemical methods. These are highly costly and even though dyes are separated, accumulation of concentrated sludge poses disposal problem. Contaminated wastewater can be effectively treated to separate dye by adsorption. This method can be economical as it does not involve any additional pre-treatment when low-cost adsorbents are used. As the material is cheap and locally available it can be a better substitute for activated carbon (Crini 2006).

Clay as an adsorbent is drawing the attention in recent years for removing dyes from wastewater (Alkan *et al*., 2007; Vimonses *et al*., 2009). Its advantages over other adsorbents are low-cost,

Corresponding author:* **Akheel Ahmed Syed
Department of Studies in Chemistry, University of Mysore, Manasagangothri, Mysore - 570006, India

availability in abundance, high adsorption rate, free from toxicity and high capability for ion exchange. These qualities are due to the net negative charge on the structure of the minerals. Use of the clays can bring large economic and environmental benefits to wastewater industries.

Several studies were done on adsorption of organic cationic dyes by clay minerals (Ghosh & Bhattacharyya 2002). But the information on adsorption of anionic dyes is very limited (Bulut *et al*., 2008). In majority of cases, adsorption capacity of acidic dyes is for lower than basic dyes. This is due to weak interactions between the negatively charge on the surface of clay minerals and anionic charge of dyes.

Kaolinite is a good adsorbent. It is available in abundance in soils and sediments and it is capable of interacting with other elements of soil for mechanical stability of the soil column. The adsorption capacity of kaolinite is decided by its surface structure and the edges (Miranda-Trevino & Coles 2003; Schoonheydt & Johnston 2006). The edges have varying charge and it can be correlated with the reaction between ionizable surface groups on the edges and the clay surface and the ions of aqueous solution. Direct Red 13 (DR13) is a bisazo dye whose application is mainly in for cotton and glue dyeing as also printing. It is also used in silk, polyamide, viscose/polyamide fiber blended fabric dyeing and widely used to color, leather and paper. DR13 is an anionic dye with comparable structure as that of Congo red. Its metabolized product is benzidine, which is a known human carcinogen. Treatment of DR13 in wastewater is not that easy, as the dye is usually present as sodium salt imparting high water soluble property. Due to its structure it is difficult to either biodegrade or photodegrade the dye. In the present paper, the first-ever study done on the use of kaolinite for the removal of Direct Red 13 dye from water by the process of adsorption has been reported.

Our research school is the first to report the use of NIS as filler material in the fabrication of thermoplastic and thermoset composites (Taqui *et al*., 2018; Syed & Syed 2016; Syed & Syed 2016a; Syed & Syed 2012; Pashaei *et al*., 2011; Syed *et al*., 2011; Syed *et al*., 2010; Syed *et al*., 2010a; Syed *et al*., 2009) and as effective adsorbents for remediation of Congo red, methylene blue and ethidium bromide dyes (Taqui *et al*., 2017; Papegowda & Syed 2017; Sulthana *et al*., 2017). Despite myriad research papers have reported the use of low–cost agriculture waste as biosorbent for the remediation of toxic dyes; a very little information is available on the use of dye adsorbed biosorbent commonly known as "sludge". We have reported on the use of "sludge" as filler material for the fabrication of thermoplastics and thermosets (Taqui *et al*. 2017; Taqui *et al*. 2018). Research is in progress to use dye-adsorbed clay minerals as filler/reinforcement material.

MATERIAL AND METHODS

Materials

Direct Red 13 (DR13) dye is soluble in water and ethanol producing wine red and red color respectively. It is insoluble in many organic solvents.[C.I. = 22155; CAS registry number =1937-35-5; chemical formula = $C_{32}H_{22}N_6Na_2O_7S_2$; molecular weight = 712.66; absorbance maximum (λ_{max}) = 503nm]. The molecular structure of the dye is shown in Figure 1.

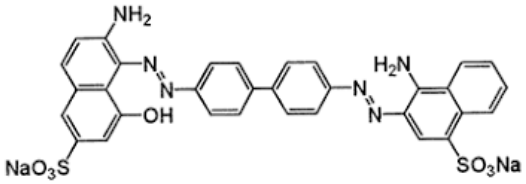

Figure 1 Structure of Direct Red 13 dye

Kaolinite was procured from Sd Fine-chem Limited, India and it was heated at 373 K for 8 h before use. UV-v is spectrometer (Perkin-Elmer Lambda EZ-201) was used to determine initial and residual concentrations of Direct Red 13 dye (Aldrich, USA) at 503 nm λ_{max}. pH was measured by a pH meter (Systronics -802, India). FTIR spectrophotometer (Perkin Elmer 3 lambda) was used to record IR spectra. Scanning electron micrograph (SEM) was done by a scanning electron microscope (JEOL model 3300). Kaolinite chemical composition was done by standard method (Solgic and Marjanovic-Krajovan, 1968). Determination of point of zero charge (pHZ) was done to assess the surface charge of kaolinite. For pHZ determination, stock solution of 0.1 M KCl was prepared; 50 ml of 0.1 M KCl were transferred to seven different 250 ml Erlenmeyer flasks. Solution pH was initially adjusted between 2.0 and 12.0 by using HCl and NaOH; 0.05 g of kaolinite was added to each solution. These flasks were continued for 24 h and the final pH of the solutions was measured using a pH meter. Graph of pH_{final} versus $pH_{initial}$ was plotted (Cardenas *et al*., 2012).

Adsorption experiments

For preparing stock solution of DR13 (1000 mg/L) double distilled water was used. Required solution concentrations (25–300 mg/L) were made by diluting the stock solution. Hence studies were carried out by batch method. Adsorption process permitted for evaluation of each parameter influencing the adsorption process. 50 mg of kaolinite taken in 250 mL conical flasks were added to 50 mL of solution DR13 (25–300 mg/L). Solution was subjected to stirring in a thermostatic orbital-shaker 165 rpm/min for 180 min. Samples were withdrawn at predetermined equilibrium time. The unadsorbed DR13 solution was separated by centrifugation. The equilibrium concentration of the DR13 pertaining to the centrifuged solution was spectrophotometrically determined. For kinetic studies of DR13 solution (100 mg/L), three temperatures (303, 313 and 323 K) were selected and experiments carried out as a function of equilibrium time (60 min). For initial solution pH effect, adsorption studies were carried out in pH range 2-12. pH was controlled at required level by adding either dilute HCl or NaOH (both 0.01 M). Experiments were replicated thrice and the mean values are considered.

Statistical optimization of process parameters

Six factors influencing the adsorption process on the final adsorption capacity were studied and these included: adsorption time (A), process temperature (B), initial dye concentration (C), particle size (D) adsorbent dosage (E) and initial pH (F). These

were the independent variables which were to be optimized arriving at for adsorption capacity which is the dependent response variable at fixed orbital shaking at 165 rpm. A standard experimental design was prepared comprising six factors at two levels (Table1). Analysis of variance (ANOVA) calculated and based on the results a general quadratic regression equation was prepared. Surface and contour plots were prepared to indicate the individual as well as interaction effects of different parameters on the adsorption process and dye uptake.

RESULTS AND DISCUSSION

Characterization of the adsorbent

Surface characterization

Scanning electron microscope (SEM) depicts different sized particles with rough edges, because of which there is much larger surface area for DR13 adsorption (Figure 2a). At the end of adsorption process, the surface area gets covered with adsorbed DR13 molecules as depicted in Figure 2b. The kaolinite FTIR spectrum displayed adsorption bands at 3640 and 3578 cm^{-1} which are attributed to hydroxyl groups and adsorbed water molecule. The peaks at 1120, 1050 and 812 cm^{-1} are attributed to C-O-C stretching. After adsorption the characteristic bands due to OH groups gets shifted from its position to 3449 and 3675 cm^{-1} indicating strong adsorption of DR13 onto kaolinite (Figure 3). Determination of point of zero charge in the intersection of two plots (Figure 4) confirms that at pH 7.9 the surface of the adsorbent is having zero charge.

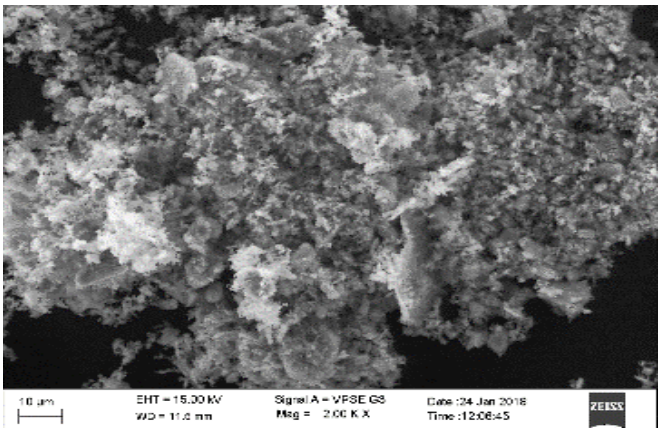

Figure 2a SEM before adsorption

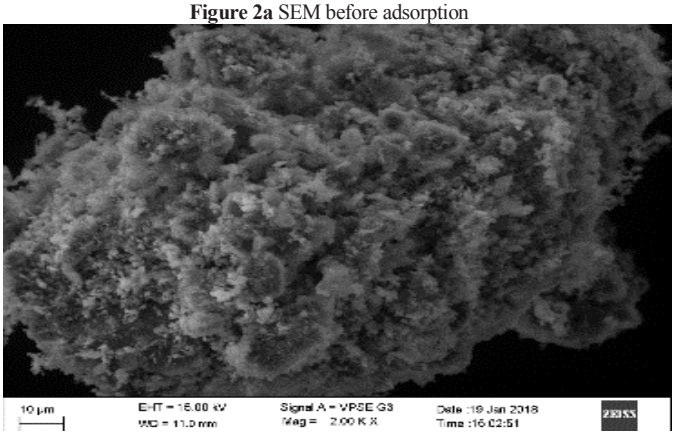

Figure2b SEM after adsorption

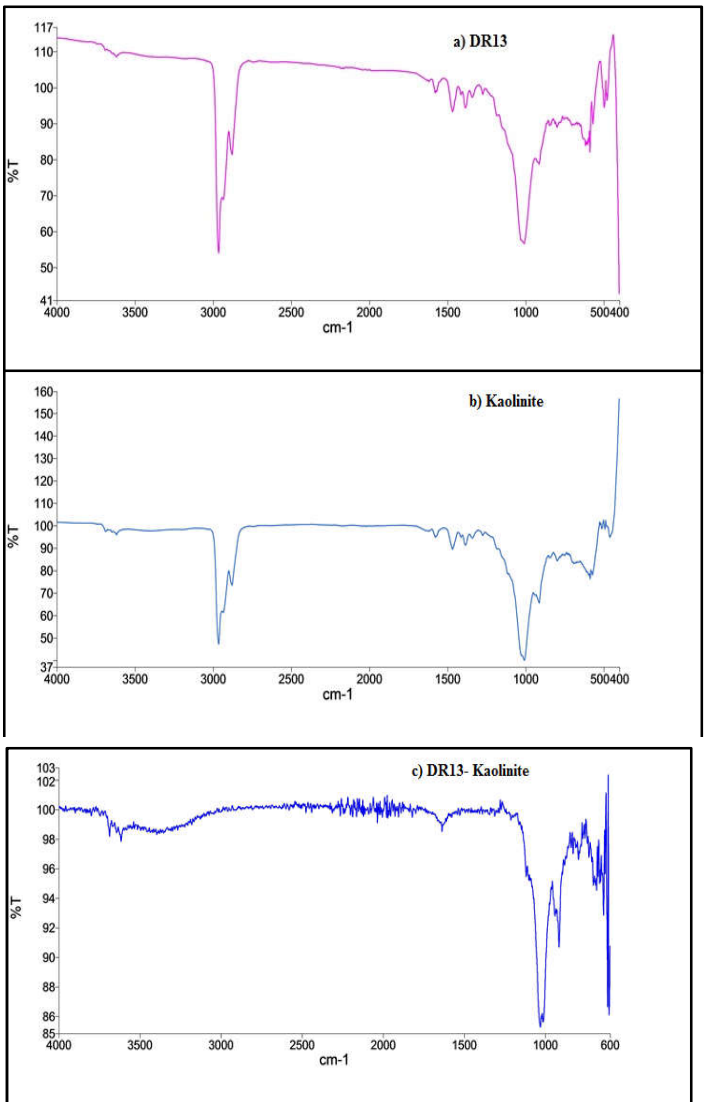

Figure 3 FTIR spectra of a) DR13 b) kaolinite c) DR13 adsorbed on kaolinite

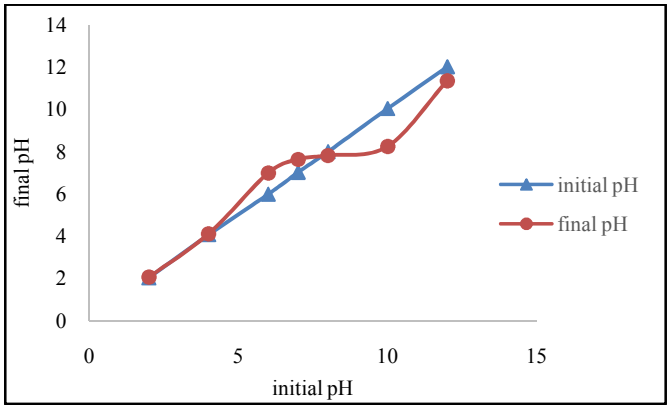

Figure 4 Point of zero charge of kaolinite at the intersection

Batch Adsorption Studies

Effect of initial dye concentration

The effect of the initial concentration of DR13 on its adsorption onto kaolinite (0.500 g/L, temperature 303 K) was studied for 180 min. Increase in the adsorption of the dye in the initial stage followed by decrease in adsorption percentage from 20 to 2 when the initial dye concentration increased from 25 to 300 mg/L (Figure 5a). Thus, it is

evident that the adsorption is dependent on initial DR13 concentration. The probable reason being that at lower concentration, the ratio of initial DR13 molecules available to the surface area was low; but later on the fractional adsorption tended to be independent of initial concentration. When concentration was high, more number of DR13 molecules had contact with the adsorption sites, which, resulted in higher number of dye molecules getting adsorbed. Thus, q_e percent value increased at the same time adsorption decreased (Figure 5a). The quantum of DR13 adsorbed was 13 mg/g at the concentration 100 mg/L.

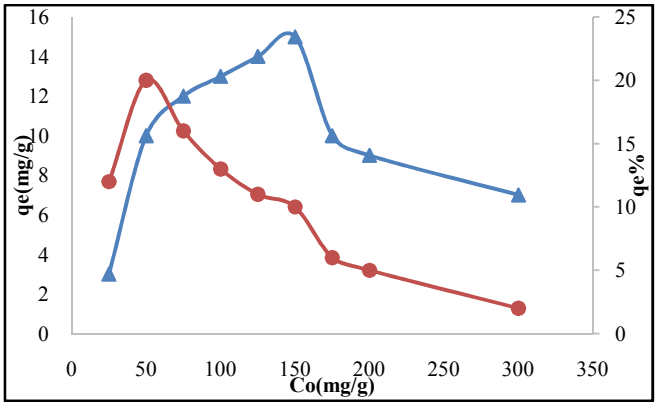

Figure 5a Effect of initial dye concentrationon DR13 adsorption by Kaolinite

Effect of dosage

To evaluate the DR13 dye adsorption capacity by kaolinite (50 mg/L, pH 7, temperature 303 K), the kaolinite dose was varied from 0.025 to 0.300 g per 50 ml of adsorbent. There was a decrease in adsorption capacity with increase in adsorbate dosage (Figure 5b). This could be due to more adsorbent surface area and availability of increased number of adsorption sites. But, there was negligible decrease in dye up take, which could be attributed to agglomerates formation of clay minerals thereby decreasing the surface area available and blocking of some adsorption sites.

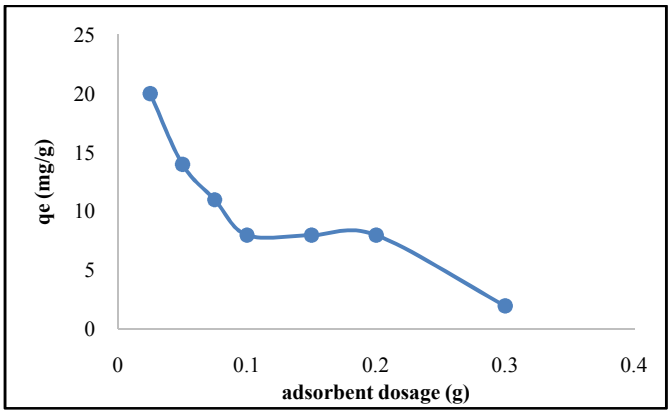

Figure 5b Effect of adsorbent dosage on adsorption of DR13

Effect ofpH on adsorption of DR13

DR13 (100 mg/L) adsorption onto kaolinite (1.000 g/L, 303 K) as a function of changing initial pH (2–12) is depicted in Figure 5c. The percent DR13 dye adsorbed decreases with increase in pH from 2 to 7 then gradually adsorption increases. The reason for this may be the surface charge of the kaolinite. The main kaolinite constituents are Al and Si oxides, which form their respective hydroxide complexes in solution. The acidic or basic dissociation of these complexes at the solid-solution interface is responsible for the development of positive or negative charge on the surface. The surface charge of surrounding oxide particles are influenced by the solution pH. It is likely that in basic media, the surfaces are negatively charged due to the presence of OH^- ions on adsorbent, and these cause electrostatic attraction between the negatively charged surface of adsorbent and the cationic DR13 dye. This may be the reason for maximum removal of DR13 dye by kaolinite taking place at pH 9. Such observation was also reported by others for the adsorption of basic dyes (Doğan *et al*., 2000). Although maximum adsorption occurred at pH 2 and pH 12, neutral pH was selected for further studies because, all water resources have range of pH 6–8.

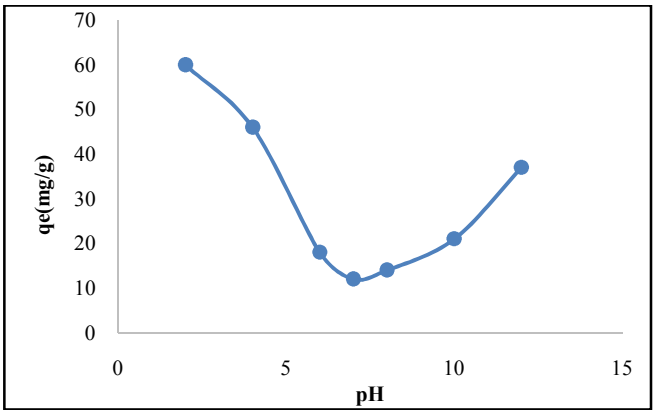

Figure 5c Effect of pH on adsorption of DR13

Effect of temperature

The percent adsorption of DR13 on to kaolinite (Figure 5d) enhanced with increase in temperature from 303 to 323 K, which indicated the endothermic property in adsorption. This could be as cribbed to; (a) that the diffusion rate of adsorbate molecules increased across the external boundary layer and the internal pores present in the adsorbent, (b) an enhancement in porosity as well as in total pore volume of the adsorbent due to temperature effect, and(c)availability of more activesites for adsorption (Srivastava & Rupainwar 2009). But, all further experiments were conducted at 303 K since most water sources are available at this temperature range.

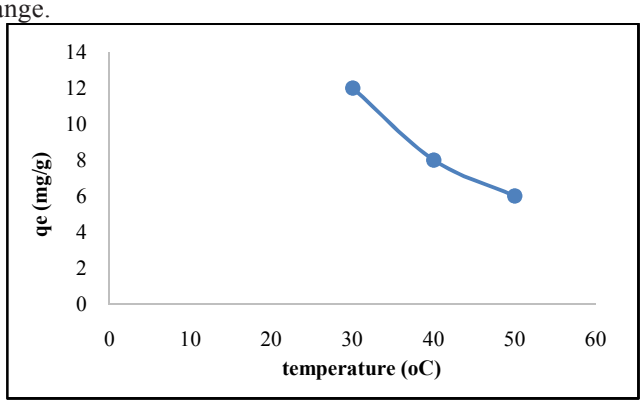

Figure 5d Effect of temperature

Adsorptionisotherms

The data on adsorption of DR13 by kaolinite were further analyzed with the help of Langmuir, Freundlich, and Temkin isotherm models.

Langmuirisotherm

The validity of this isotherm is for monolayer adsorption. The below equation (1) represents the linearized form (Langmuir 1918):

$$C_e/q_e = 1/(bQ_m) + (1/Q_m)\,Ce \quad (1)$$

Here, C_e is the equilibrium concentration of DR13 in solution, q_e is quantum of DR13 adsorbed at equilibrium, $Q_m$is monolayer adsorption capacity of Langmuir, and b is Langmuir constant with respect to equilibrium constant of adsorption (dye + Clay = dye – clay equilibrium). As can be observed from Figure 6a, the plots of C_e/q_e versus Ce at varying temperatures (303, 313 and 323 K) are linear, which indicates that the adsorption is according to Langmuir isotherm model. The slope and the intercept in the linear plots provide Q_m and b values, respectively. The Langmuir constant values along with the R^2 values are provided in Table 1.

The present adsorption capacity (Q_m) result of kaolinite (13 mg/g) is higher compared to other adsorbents reported earlier. These include 8.5 mg/g for banana pith (Namasivayam *et al*., 1993), 1.18 mg/g for fly ash (Khan *et al*., 2004), 3.94 mg/g for tamarind fruit shell carbon (Vasu 2008), 10.67 mg/g for pandanus leave carbon (Hema & Arivoli 2007).

Freundlich isotherm

Freundlich isotherm equation, describes non-specific adsorption, and it has been applied to interpret adsorption data. Freundlich equation(Eq.2) in its linear form is given below (Freundlich 1906):

$$\log q_e = \log K_f + n \log C_e \quad (2)$$

Where, K_f is Freundlich coefficient which describes adsorption capacity and n is adsorption intensity. The arc obtained by the slope and intercept of the linearized plots (log q_e *versus* logC_e, Figure 6b). $K_f$and n values as well as correlation coefficient (R^2) are given in Table 1. The values of n lying between 0.48 and 0.69 indicate that the process favors physical adsorption.

Temkin isotherm

Temkin isotherm (Eq.3) assumes that the heat of adsorption o fall the molecules in the layer decreases linearly due to adsorbate-adsorbent interactions, and adsorption is characterized by a uniform distribution of binding energies, up to some maximum binding energy (Temkin & Pyzhev1940). The equation is

$$Q_m = RT/blnA + RT/blnC_e, with\ B = RT/b \quad (3)$$

Where, Q_m is adsorption capacity(mg/g), C_e is equilibrium dye concentration (mg/L).A and B are Temkin constants, related to equilibrium binding constant and heat of adsorption, respectively. The linear plot of q_e versus $ln\ C_e$ (Figure 6c) at different temperatures (303, 313 and 323 K) gave a good fit for the Temkin isotherm with R2 value being 0.094. Temkin constants and R2 values are provided in Table 1.

The best fit among the isotherm models can be determined by comparing the correlation factors of all isotherm models studied as shown in Table 1. The correlation coefficients for Langmuir model is 0.87 which is highest when compared to Freundlich 0.19 and Temkin 0.094. Hence, Langmuir isotherm can be considered as the best fit adsorption of DR13 dye onto kaolinite.

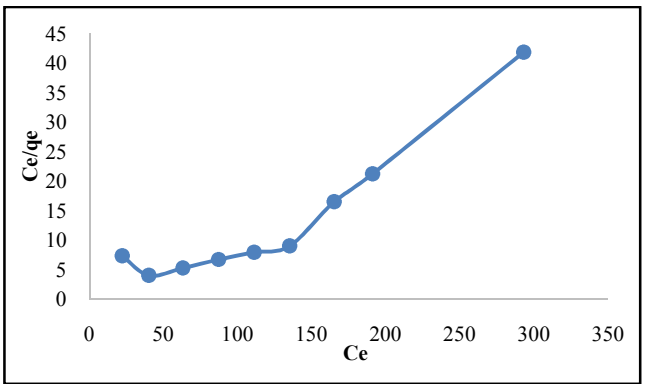

Figure 6a Fitting of adsorption data to Langmuir adsorption isotherm

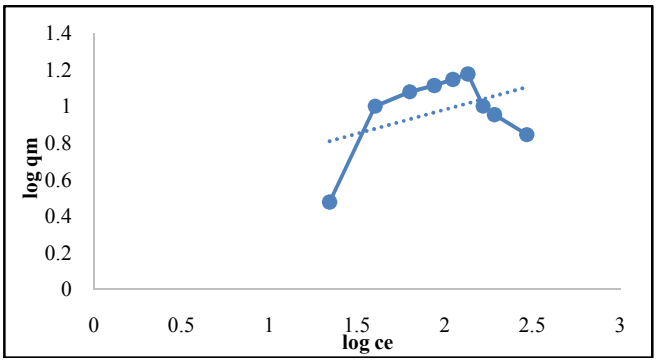

Figure 6b Fitting of adsorption data to Freundlich adsorption isotherm

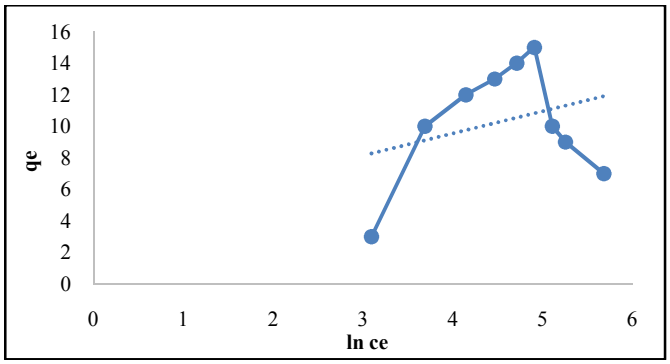

Figure 6c Fitting of adsorption data to Temkin adsorption isotherm

Table 1 Adsorption isotherm constants and correlation coefficients

	Langmuir isotherm		Freundlich isotherm			Temkin isotherm		
Q_m	b	R^2	K_F	n	R^2	A	B	R^2
7.535	0.0441	0.8685	2.865	0.263	0.1879	319.153	1.4098	0.0936

Adsorption Kinetics

In adsorption process, analysis of the kinetic data is important since the kinetics describe the uptake rate of adsorbate which helps to predict the mechanism of sorption and rate controlling

steps. In the present investigation, pseudo- first order and pseudo- second order models were used for testing the experimental data.

Pseudo-first order kinetic model

The differential rate equation is in the form:

$$dq_t/d_t = k_1 (q_e - q_t) \quad (4)$$

where, q_t and q_e are the amounts of dye adsorbed at time t (mg/g) and at equilibrium (mg/g), respectively and k1 is the pseudo-first order rate constant (min^{-1}). Integrating the above equation using the boundary condition, $q_t = 0$ at $t = 0$.

$$log (q_e - q_t) = log\ q_e - (k1/2.303)\ t \quad (5)$$

The values of k_1 and q_e were calculated from the slopes and intercepts of the linear plots of $log(q_e - q_t)$ versust (Figure 7a), respectively and presented in Table 2.

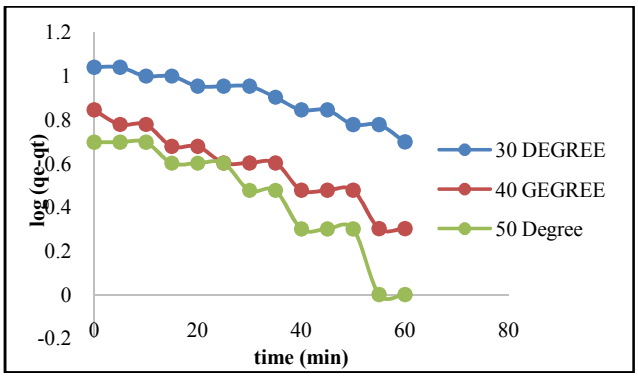

Figure 7a Pseudo first order kinetic model of DR13 on kaolinite system at different temperatures

Pseudo-second order kinetic model

The pseudo-second order kinetic model is presented as:

$$dqt/dt = k_2 (q_e - q_t)2 \quad (6)$$

Where q_t and q_e are the amount of dye adsorbed at time t (mg/g) and at equilibrium (mg/g), respectively and k_2 is the pseudo-second order rate constant (g/mg/min). Integrating the above equation using the boundary condition, $q_t = 0$ at $t = 0$ leads to:

$$t/qt = 1/k_2\ qe^2 + t/\ q_e \quad (7)$$

The values of k_2 and q_e were calculated from intercepts and slopes of the linear plots of t/q_tversust (Figure 7b), respectively and presented in Table 2 which shows that the calculated q_e values are very close to that of experimentally obtained qe and the values of correlation coefficients (R^2) are closer to unity confirming that adsorption of DR13 on kaolinite follows pseudo-first order kinetics.

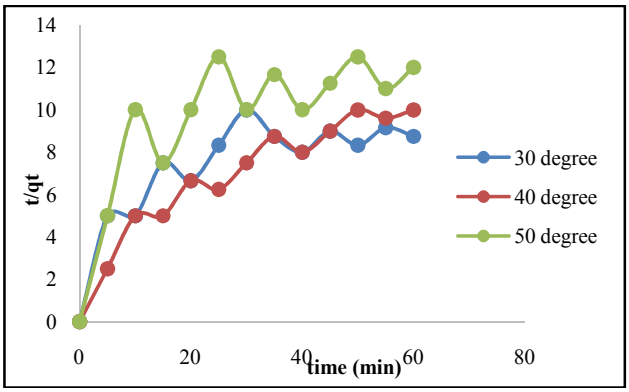

Figure 7b Pseudo second order kinetic model of DR13 on kaolinite system at different temperatures

Table 2 Experimentally determine and theoretically predicted parameters for adsorption kinetic models

Temperature (K)	Initial dye Concentration (mg/L)	$q_e$exp	Pseudo-first order			Pseudo-second order		
			Q_m cal	k_1	R^2	Q_m cal	k_2	R^2
303	100	12	11.795	0.0126	0.9487	9.661	$2.5745*10^{-3}$	0.5755
313	100	08	6.956	0.0198	0.9515	6.854	$8.8170*10^{-3}$	0.8762
323	100	06	7.910	0.0276	0.8982	7.434	$3.3155*10^{-3}$	0.5499

Statistical optimization by Response Surface Methodology (RSM) using Fractional Factorial Experimental Design (FFED)

Adsorption time (A), process temperature (B), initial dye concentration (C), adsorbent dosage (D) and initial pH (E) were chosen as independent variables to optimize the adsorption capacity which is the dependent response variable at fixed orbital shaking of 165 rpm particle size of adsorbent material of 177µ. Independent variables with experimental range of an experimental design are shown in Table 3. Quadratic model in Fractional Factorial Experimental Design (FFED) under Response Surface Methodology (RSM) was used to statistically optimize the adsorption capacity. The study design of 65 experiments along with experimental and predicted values is stated in Table 4. The model can be explained by following general equation

$$Y = \beta_0 + \sum \beta_i X_i \quad (8)$$

Where Y represents the dependent response variable, β_0 is regression coefficient, $\beta_i$is the linear effect, β_{ii} is the squared effect and $\beta_{ij}$is the interaction effect of independent variable X.

Table 3 Experimental range for individual factors

Factor	Name	Units	Minimum	Maximum
A	Time	minutes	0	180
B	Temperature	^{0}C	27	50
C	Concentration	mg/L	25	500
D	Adsorbent dosage	g/L	0.500	4.000
E	pH		2	12

Table 4 FFED matrix with Experimental and Predicted Values

Standard Order	A	B	C	D	E	Actual value (%)	Predicted value (%)
1	180	27	25	0.05	7	3	7.3
2	180	27	50	0.05	7	10	10.0
3	180	27	75	0.05	7	12	12.1
4	180	27	100	0.05	7	13	13.5
5	180	27	125	0.05	7	14	14.5
6	180	27	150	0.05	7	15	14.8
7	180	27	175	0.05	7	10	14.5
8	180	27	200	0.05	7	9	13.7
9	180	27	300	0.05	7	7	4.6
10	180	27	100	0.05	2	60	64.7
11	180	27	100	0.05	4	46	35.3
12	180	27	100	0.05	6	18	17.8
13	180	27	100	0.05	7	12	13.5
14	180	27	100	0.05	8	14	12.3
15	180	27	100	0.05	10	21	18.7
16	180	27	100	0.05	12	37	37.0
17	180	27	100	0.025	7	20	15.6
18	180	27	100	0.05	7	14	13.5
19	180	27	100	0.075	7	11	11.7
20	180	27	100	0.1	7	8	10.0
21	180	27	100	0.15	7	8	7.2
22	180	27	100	0.2	7	8	5.1
23	180	27	100	0.3	7	2	3.1
24	180	30	100	0.05	7	12	12.7
25	180	40	100	0.05	7	8	9.3
26	180	50	100	0.05	7	6	5.4
27	0	30	100	0.05	7	1	0.5
28	5	30	100	0.05	7	1	1.1
29	10	30	100	0.05	7	2	1.7
30	15	30	100	0.05	7	2	2.3
31	20	30	100	0.05	7	3	2.8
32	25	30	100	0.05	7	3	3.4
33	30	30	100	0.05	7	3	3.9
34	35	30	100	0.05	7	4	4.4
35	40	30	100	0.05	7	5	4.9
36	45	30	100	0.05	7	5	5.4
37	50	30	100	0.05	7	6	5.9
38	55	30	100	0.05	7	6	6.3
39	60	30	100	0.05	7	7	6.8
40	0	40	100	0.05	7	1	1.0
41	5	40	100	0.05	7	2	1.5
42	10	40	100	0.05	7	2	2.0
43	15	40	100	0.05	7	3	2.5
44	20	40	100	0.05	7	3	2.9
45	25	40	100	0.05	7	4	3.4
46	30	40	100	0.05	7	4	3.8
47	35	40	100	0.05	7	4	4.2
48	40	40	100	0.05	7	5	4.6
49	45	40	100	0.05	7	5	5.0
50	50	40	100	0.05	7	5	5.3
51	55	40	100	0.05	7	6	5.7
52	60	40	100	0.05	7	6	6.0
53	0	50	100	0.05	7	1	0.9
54	5	50	100	0.05	7	1	1.3
55	10	50	100	0.05	7	1	1.7
56	15	50	100	0.05	7	2	2.0
57	20	50	100	0.05	7	2	2.4
58	25	50	100	0.05	7	2	2.7
59	30	50	100	0.05	7	3	3.0
60	35	50	100	0.05	7	3	3.3
61	40	50	100	0.05	7	4	3.6
62	45	50	100	0.05	7	4	3.9
63	50	50	100	0.05	7	4	4.1
64	55	50	100	0.05	7	5	4.4
65	60	50	100	0.05	7	5	4.6

RESULTS AND DISCUSSION

Experiments were carried out with different combinations of six independent variables to study the individual as well as combined effects. ANOVA (Table 5) obtained from the quadratic regression analysis shows that the individual and combined effects of these factors are significant. Significance was considered at ≤ 0.05. In this study A, B, D, E, AB, A^2, C^2, andE^2 are significant model terms and other variables are insignificant. Cross products AD, AE, BD, BE, CD, CE, DE and EF are zero and hence are excluded to construct the regression equation. The RSM model is highly significant with model F-Value of 118.90. High R^2 value of 96.10% with insignificant lack-of-fit and coefficient of variance (CV) of 26.90% assure that model can be used to navigate the design space. The comparison graph for actual *versus* predicted values (Figure 8) indicate a strong relationship between the experimental and predicted responses. The regression equation obtained from the study is shown in the following equation (Eq-9)

Adsorption=2.2+4.5*A-1.9*B-1.4*C-6.2D-13.9*E-2.2*AB -2.5*A^2-0.4*B^2-8.8*C^2 +2.7*D^2 +37.3*E^2 (9)

Table 5 ANOVA for fractional factorial experimental design

Source	Sum of Squares	Degree of freedom	Mean Square	F Value	P- Value
Model	6368.3	11	578.9	118.9	< 0.001**
A	271.3	1	271.3	55.7	< 0.001**
B	65.9	1	65.9	13.5	< 0.001**
C	6.3	1	6.3	1.3	0.2619
D	159.4	1	159.4	32.7	< 0.001**
E	537.7	1	537.7	110.4	< 0.001**
AB	48.7	1	48.7	10.0	0.003**
A^2	24.9	1	24.9	5.1	0.0279*
B^2	1.0	1	1.0	0.2	0.6486
C^2	113.4	1	113.4	23.3	< 0.001**
D^2	8.3	1	8.3	1.7	0.1967
E^2	2538.0	1	2538.0	521.2	< 0.001**
Residual	258.1	53	4.9		
Lack of fit	256.1	51	5.0	5.0	0.1799
Total	6626.4	64			

Significant figures
+ Suggestive significance (p value: 0.05 <p <0.10)
* Moderately significant (p value: 0.01 <p≤ 0.05)
** Strongly significant (p value: $p \leq 0.01$)

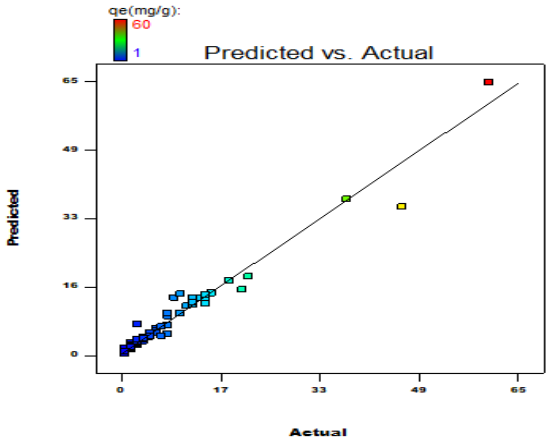

Figure 8 Comparison graph for actual versus predicted values

The optimal values of the variables determined by maximization of the second-order polynomial equation with interaction terms obtained by multiple regression analysis based on FFED. Maximum adsorption obtained by the statistical optimization experiment was 85mg/g with optimized conditions established as a pH of 1, adsorbent dosage of 0.600 g/L, and particle size of 177µ and an initial dye concentration

of 119 mg/L for an adsorption time of 164 min with orbital shaking of 165 rpm at temperature 30.5°C.

Finally the analysis of 3D response surface plots and contour plots was done as a function of two independent variables, which determined the interaction between two parameters keeping all others at a constant value.

Statistical process optimization, in a given range of parameter values, allows not only for calculating the optimal condition, but also for determining the effect of the process conditions on adsorption. 3D graphs (Figures 9-12) plotted for time against all other factors indicate that time has a positive effect on adsorption capacity. By increasing time along with particle size and dye concentration, it is possible to increase the process of adsorption. Maximum time of 165 min has shown maximum adsorption. Increase in temperature from 27°C to 30°C has increased the adsorption capacity. Increase beyond 31°C, decreases the adsorption capacity. Increase in pH beyond 2 decreases adsorption capacity even if time is increased. Graph (Figure 11) plotted time and adsorbent dosage indicates that absorbent dosage has negative effect on adsorption. However, increased time can improve the process of adsorption. Graphs (Figures 13-15) for temperature against other independent variables indicate that temperature has negative effect with all other variables on the response. Graphs (Figures 16-17) plotted for initial dye concentration against other variables indicate that increase in the initial concentration have positive effect for adsorption capacity. Graph (Figure 18) plotted against pH and adsorbent dosage indicates that absorbent dosage has negative effect on adsorption process. Maximum adsorption was observed at concentration of 120 g/L beyond which it has a negative effect.

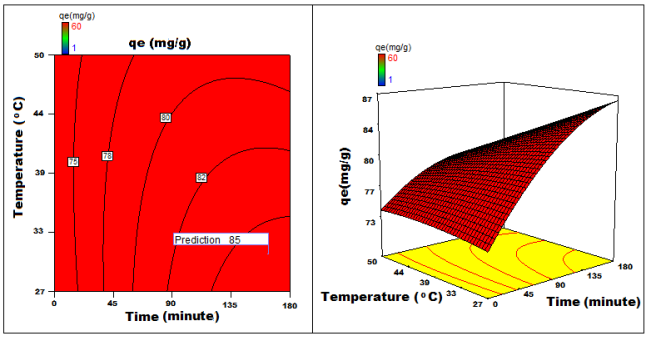

Figure 9 3D surface plot and contour plot showing the variation of adsorption capacity with timeversus temperature

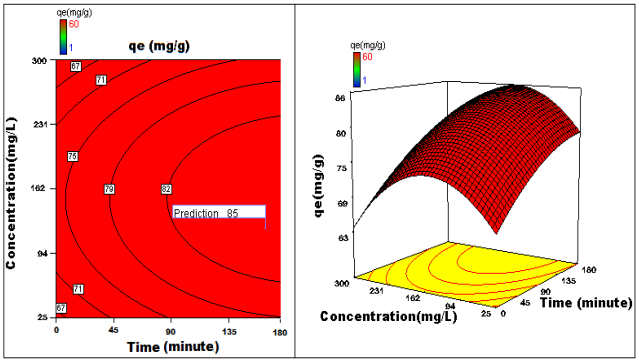

Figure 10 3D surface plot and contour plot showing the variation of adsorption capacity with time versus concentration

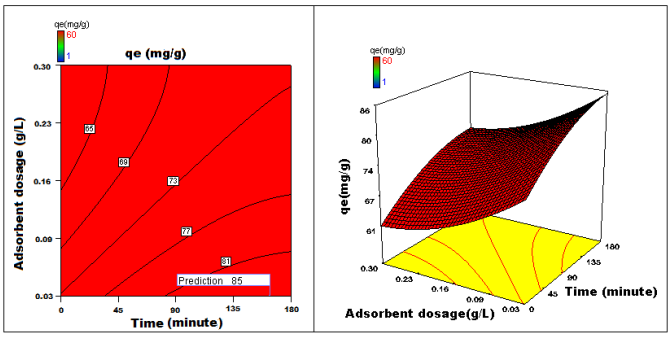

Figure 11 3D surface plot and contour plot showing the variation of adsorption capacity with time versus adsorbent dosage

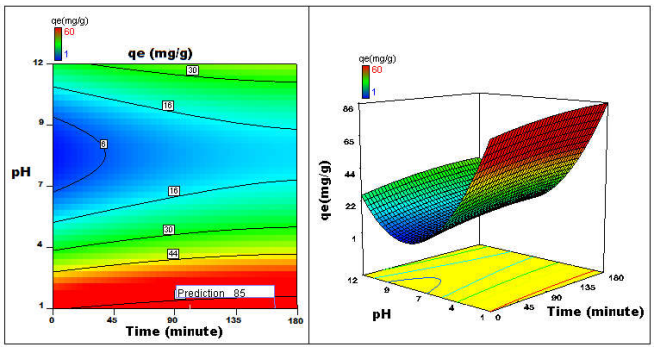

Figure 12 3D surface plot and contour plot showing the variation of adsorption capacity with time versus pH

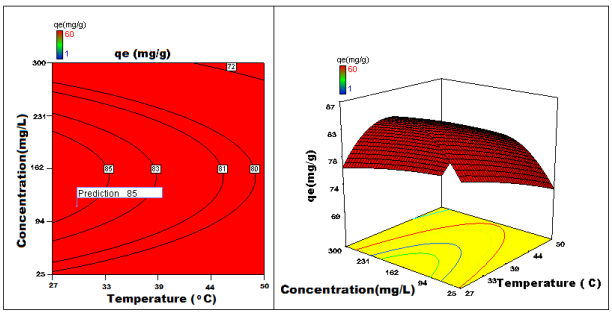

Figure 13 3D surface plot and contour plot showing the variation of adsorption capacity with temperature versus concentration

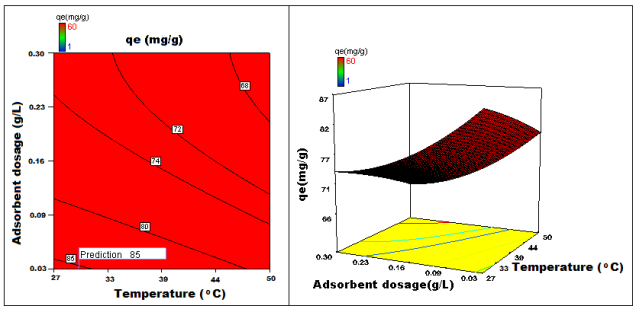

Figure 14 3D surface plot and contour plot showing the variation of adsorption capacity with Temperature versus Adsorbent dosage

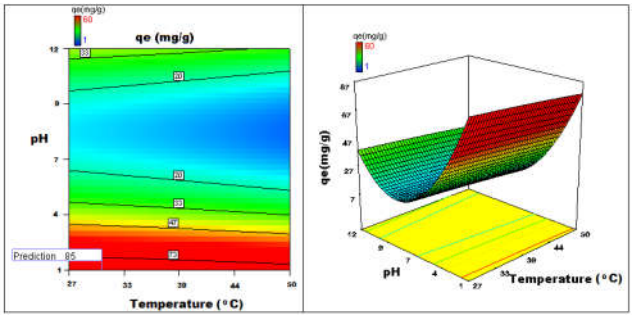

Figure 15 3D surface plot and contour plot showing the variation of adsorption capacity with temperature versus pH

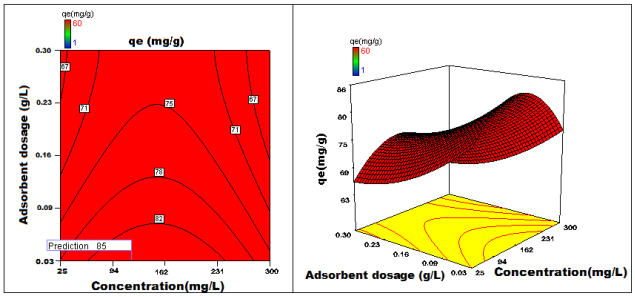

Figure 16 3D surface plot and contour plot showing the variation of adsorption capacity with adsorbent dosage versus concentration

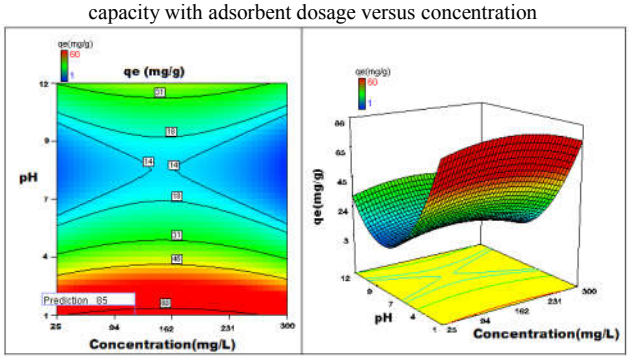

Figure 17 3D surface plot and contour plot showing the variation of adsorption capacity with pH versus concentration

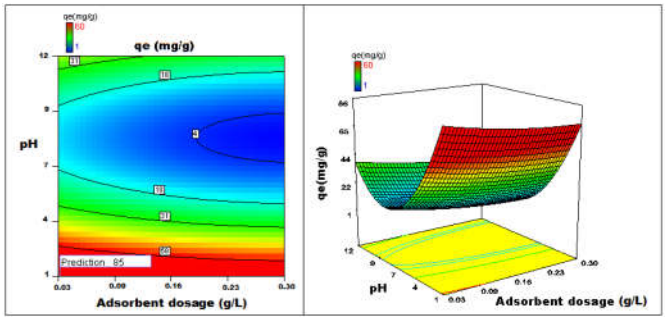

Figure 18 3D surface plot and contour plot showing the variation of sorption capacity with adsorbent dosage versus pH

The quadratic model developed for process optimization is found to be benifical for predicting the maximum adsorption capacity and understanding the interaction between independent variables as well as their effect on adsorption process. From statistical optimization there is almost 41.70% increase in adsorption from 60 mg/gto 85 mg/g.

CONCLUSION

Kaolinite has shown as an effective adsorbent in the removal of DR13 dye from aqueous solution. This is due to low adsorption time, good adsorption capacity compared to many of low-cost agriculture waste materials used. The process of adsorption of DR13 dye by the adsorbent was almost spontaneous and endothermic. Analysis of variance proved that DR13 dye uptake by kaolinite was influenced by initial dye concentration, pH, dosage and temperature. Dye binding on the surface of kaolinite is evident by the FTIR spectra of the kaolinite. Isotherm data fitted to Langmuir model. These preliminary results will direct us for up-scaling of the process and for removal of DR13 dye from the effluents.

Acknowledgment

One of the authors (MAHDA) gratefully acknowledges Thamar University, Republic of Yemen for the award of Overseas Research Fellowship.

References

Alkan, M., Demirbaş, Ö.,& Doğan, M. (2007). Adsorption kinetics and thermodynamics of an anionic dye onto sepiolite. *Microporous and Mesoporous Materials*, 101(3), 388-396.

Bafana, A., Devi, S. S., & Chakrabarti, T. (2011). Azo dyes:past, present and the future. *Environmental Reviews*, 19, 350-371.

Bulut, E., Özacar, M., &Şengil, İ. A. (2008). Equilibrium and kinetic data and process design for adsorption of Congo Red onto bentonite. *Journal of hazardous materials*,154(1-3), 613-622.

Cardenas, P.A.M., Ibanez, J.G., & Vasquez, M.R. (2012). Determination of the point of zero charge for electrocoagulation precipitates from an iron anode. *International Journal of Electrochemical Science*, 7, 6142--6153.

Crini, G. (2006). Non-conventional low-cost adsorbents for dye removal: a review. *Bioresource Technology*, 97(9), 1061-1085.

Doğan, M., Alkan, M., & Onganer, Y. (2000).Adsorption of methylene blue from aqueous solution onto perlite. *Water, Air, and Soil Pollution,* 120(3-4), 229-248.

Freundlich, HMF. (1906). Over the adsorption in solution. *Journal of Phyical Chemistry*, 57, 385-471.

Ghosh, D., & Bhattacharyya, K. G. (2002).Adsorption of methylene blue on kaolinite. *Applied Clay Science*, 20(6), 295-300.

Hema, M., &Arivoli, S. (2007). Comparative study on the adsorption kinetics and thermodynamics of dyes onto acid activated low cost carbon. *International Journal of Physical Sciences*, 2(1), 10-17.

Hubbe, M. A., Hasan, S. H., & Ducoste, J. J. (2011).Cellulosic substrates for removal of pollutants from aqueous systems: A review. 1. Metals. *Bio Resources*,6(2),2161-2287.

Khan, M. J., Al-Juhani, A. A., Shawabkeh, R., Ul-Hamid, A., & Hussein, I. A. (2011).Chemical modification of waste oil fly ash for improved mechanical and thermal properties of low density polyethylene composites. *Journal of Polymer Research*, 18(6), 2275-2284.

Langmuir, I. (1916). The constitution and fundamental properties of solids and liquids.*Journal of the American Chemical Society*, 38(11), 2221-2295.

Miranda-Trevino, J. C., & Coles, C. A. (2003).Kaolinite properties, structure and influence of metal retention on pH. Applied Clay Science, 23(1-4), 133-139.

Namasivayam, C., &Periasamy, K. (1993).Bicarbonate-treated peanut hull carbon for mercury (II) removal from aqueous solution. *Water Research*, 27(11), 1663-1668.

Papegowda, P. K., & Syed, A. A. (2017). Isotherm, Kineticand Thermodynamic Studies on the Removal of Methylene Blue Dye from Aqueous Solution Using Saw Palmetto Spent. *International Journal of Environmental Research*, 11(1), 91-98.

Pashaei, S., Siddaramaiah, & Syed, A. A. (2011).Investigation on mechanical, thermal and morphological behaviors of turmeric spent incorporated vinyl ester green composites. *Polymer-Plastics Technology and Engineering,* 50(12), 1187-1198.

Schoonheydt, R. A., & Johnston, C. T. (2006). Surface and interface chemistry of clay minerals. *Developments in Clay Science*, 1, 87-113.

Solgic, Z., & Marjanovic-Krajovan, Y. (1968). Méthoderapided'analyse de SiO_2Fe, 2, 122-127.

Srivastava, R., & Rupainwar, D. C. (2009). Eucalyptus bark powder as an effective adsorbent: Evaluation of adsorptive characteristics for various dyes. *Desalination and Water Treatment,* 11(1-3), 302-313.

Sulthana, R., Taqui, S.N., Zameer, F., Taqui, S.U., and Syed, A.A. (2017). Adsorption of ethidium bromide from aqueous solution on to nutraceutical industrial fennel seed spent: Kinetics and thermodynamics modeling Studies. *International Journal of Phytoremediation*, doi10.1080/15226514.2017.1365331.

Syed, M. A., Siddaramaiah, Suresha, B., & Syed, A. A. (2009). Mechanical and abrasive wear behavior of coleus spent filled unsaturated polyester/polymethylmethacrylate semi interpenetrating polymer network composites. *Journal of Composite Materials*, 43(21), 2387-2400.

Syed, M. A., Ramaraj, B., Akhtar, S., & Syed, A. A. (2010).Development of environmentally friendly high density polyethylene and turmeric spent composites: Physicomechanical, thermal, and morphological studies. *Journal of Applied Polymer Science*, 118(2), 1204-1210.

Syed, M. A., Siddaramaiah, Syed, R. T., & Syed, A. A. (2010a). Investigation on Physico Mechanical Properties, Water, Thermal and Chemical Ageing of Unsaturated Polyester/Turmeric Spent Composites. *Polymer-Plastics Technology and Engineering*, 49(6), 555-559.

Syed, M. A., Akhtar, S., & Syed, A. A. (2011). Studies on the physic mechanical, thermaland morphological behaviors of high density polyethylene/coleus spentgreen composites. *Journal of Applied Polymer Science,* 119(4), 1889-1895.

Syed, M. A., & Syed, A. A. (2012). Development of a new inexpensive green thermoplastic composite and evaluation of its physico-mechanical and wear properties. *Materials & Design (1980-2015)*, 36, 421-427.

Syed, M. A., & Syed, A. A. (2016). Development of green thermoplastic composites from Centella spent and study of its physicomechanical, tribological, and morphological characteristics. *Journal of ThermoplasticComposite Materials*, 29(9), 1297-1311.

Syed, M. A., & Syed, A. A. (2016a). Investigation on physicomechanical and wear properties of new green thermoplastic composites. *Polymer Composites*, 37(8), 2306-2312.

Taqui, S. N., Yahya, R., Hassan, A., Nayak, N., & Syed, A.A. (2017). Development of sustainable dye adsorption system using nutraceutical industrial fennel seed spent—studies using Congo red dye. *International Journal of Phytoremediation*, 19(7), 686-694.

Taqui, S. N., Yahya, R., Hassan, A., Nayak, N., & Syed, A.A. (2018). A novel sustainable design to develop polypropylene and unsaturated polyester resin polymer composites from waste of major polluting industries and investigation on their physicomechanical and wear properties. *Polymer Composites*, doi:10.1002/pc.24819.

Temkin, M. J., & Pyzhev, V. (1940).Recent modifications to Langmuir isotherms. *Acta Physical Chemistry*, 12, 217-222.

Vasu, A. E. (2008). Removal of basic dyes from aqueous solutions by activated carbon prepared from Tamarindusindica fruit shells. *Oriental Journal of Chemistry*, 24(3), 947-954.

Vimonses, V., Lei, S., Jin, B., Chow, C. W., & Saint, C. (2009). Adsorption of congo red by three Australian kaolins. *Applied Clay Science*, 43(3-4), 465-472.

How to cite this article:

Mohammed A. H. Dhaif Allah and Akheel Ahmed Syed. 2018, Use of Kaolinite as an Adsorbent: Equilibrium and Dynamics of Adsorption of Direct red 13 from Aqueous Solution. *Int J Recent Sci Res.* 9(8), pp. 28260-28269.
DOI: http://dx.doi.org/10.24327/ijrsr.2018.0908.2427

****